Prediction of Harmonic Force Acting on Cantilever Beam

Bor-Tsuen Wang[1], Kuan-Yuan Lin[2]

[1] Professor [2] Graduate student
Department of Mechanical Engineering
National Pingtung University of Science and Technology
Pingtung, 91207
TAIWAN

Nomenclatures

$a(x_i,t)=a_i(t)$	predicted acceleration response of beam
$\hat{a}(x_i,t)=\hat{a}_i(t)$	measured acceleration response of beam
A	beam acceleration amplitude
A_b	the cross sectional area of beam
b_b	beam width
C_b	damping coefficient of beam
E_b	Young's Modulus of beam
$F(x,t)$	force function acting on beam
F_j	the *j*-th impact force amplitude
f_n	the *n*-th natural frequency of beam
f_s	harmonic excitation frequency
I_b	cross sectional moment of inertia of the beam
L_b	beam length
N	number of modes
N_t	number of time data points
Q_t	objective function
$q_n(t)$	modal coordinate
t_b	beam thickness
$w(x,t)$	beam lateral displacement
x_j	the location of the *j*-th harmonic force in *x*-coordinate
x_i	the location of the *i*-th accelerometer sensor in *x*-coordinate
$\omega_s=2\pi f_s$	excitation frequency
$\omega_n=2\pi f_n$	the *n*-th natural frequency of beam
ρ_b	beam density
ξ_n	the *n*-th modal damping ratio of beam
$\phi_n(x)$	the *n*-th displacement mode shape of beam
$\phi_{n,j}=\phi_n(x_j)$	the *n*-th hammer mode shape function of beam at the *j*-th location of the hammer actuator

ABSTRACT

This paper presents the force prediction for a cantilever beam subjected to harmonic excitation. With the assumption of the structural modal parameters known a priori, the acceleration response of the beam due to the harmonic excitation is also measurable and used as the input for the prediction model. The force prediction algorithm can be developed to determine the harmonic force amplitude and its location, simultaneously. The beam response excited by the harmonic force is first derived. The optimization problem to determine the harmonic force amplitude and location is then formulated. The objective function can be defined as the mean square errors between the predicted and measured acceleration response, while the design variables are identified as the force amplitude and its location number associated with the structural mode shape. Theoretical simulation is presented to demonstrate the feasibility and correctness of the developed force prediction algorithm. Experimental verification is also carried out to validate the prediction model. Results show that the harmonic force amplitude and its location can be reasonably predicted. The developed methodology can be easily extended to other structures or applied by using different kinds of sensing devices for harmonic force prediction.

Keywords: force prediction, harmonic force, cantilever beam, optimization

I. Introduction

Force prediction, identification or determination has drawn much attention for engineering design and applications. Stevens [1] gave an overview for those early-related works. Wang [2] not only provided with an extensive review about the subject but also attempted to develop a general approach in force prediction problem for arbitrary structures. The general idea of force prediction model was presented. He addressed several concerns in force prediction such as structural modeling techniques, solution methods of response estimation and types of sensors used in measuring response. The general optimization methods in determining the impact and harmonic forces were developed. This paper will modifies Wang's approach [2] in predicting the unknown harmonic force acting on a cantilever beam.

Lots of mechanical components are in harmonic excitation conditions, in particular, for rotating machineries. Such harmonically excited forces, for examples due to imbalance or hydraulic flow, may not practically measured but interested and crucial for structural design or diagnosis. Verhoeven [3] constructed synthesized transfer functions from theoretical modal analysis to estimate the excitation forces of rotating machines. Vyas and Wicks [4] adapted the similar approach to determine the turbine blade forces. Karlsson [5] presented the prediction of complex amplitudes of harmonic force by assuming the force spatial distribution available a priori.

In force prediction, the force location is also of great interest. The pattern match technique is generally adopted to search the unknown force location. Moller [6] tentatively gave the spatial shape and position of harmonic point load to match the load location. Wu et al. [7] identified the impact force location by comparing the structural response among possible candidate locations. Similarly, Choi and Chang [8] determined the impact force time history and location in two separate solution loops. Doyle and his coworkers [9-11] solved for the time history and location of impact forces separately. Recently, Wang [2] developed an optimization method in predicting the unknown impact and harmonic forces acting on arbitrary structures. The force contents including the force amplitude and its location can be determined simultaneously. Wang and Chiu [12] followed Wang's formulation [2] and experimentally showed the determination of amplitude and location of the unknown impact force acting on simply supported beam in one loop of solution. This paper slightly modifies Wang's method [2] to develop the prediction model for unknown harmonic force. Section II details the beam response analysis and the development of harmonic prediction model. Sections III and IV describe the implementation of prediction program and the experimental work, respectively. Section V shows both the theoretical and experimental prediction results, respectively, and demonstrates the feasibility of the developed force prediction model.

II. Theoretical Analysis:
2.1 Beam Response analysis

Consider a uniform cantilever beam as shown in Figure 1(a). The system equation of motion for lateral vibration analysis can be written [13]:

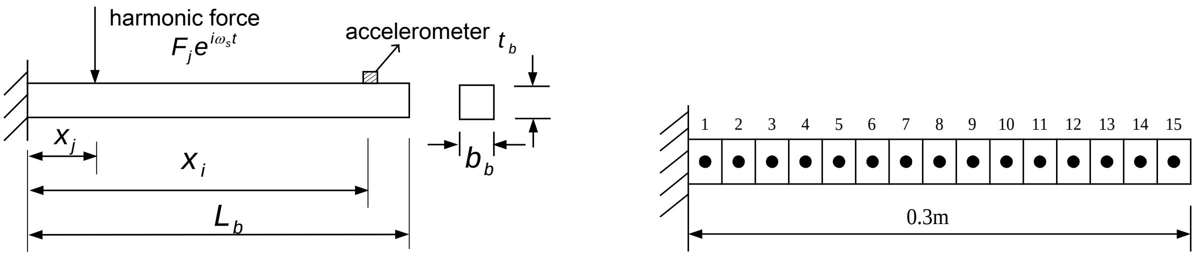

(a) system diagram **(b) test grid points**

Figure 1. Cantilever beam system diagram

$$E_b I_b \frac{\partial^4 w(x,t)}{\partial x^4} + C_b \frac{\partial w(x,t)}{\partial t} + \rho_b A_b \frac{\partial^2 w(x,t)}{\partial t^2} = F(x,t) \tag{1.}$$

If the applied force is harmonic acting at $x = x_j$, the force function can be expressed:

$$F(x,t) = F_j \delta(x - x_j) e^{i\omega_s t} \tag{2.}$$

where Delta function $\delta(x - x_j)$ represents the harmonic force location. From expansion theorem, the beam response can be assumed:

$$w(x,t) = \sum_{n=1}^{\infty} \phi_n(x) q_n(t) = \sum_{n=1}^{\infty} \phi_n(x) Q_n e^{i\omega_s t} \tag{3.}$$

By the substitution of Equation (3) into Equation (1), the beam displacement at $x = x_i$ can be derived:

$$w(x_i,t) = \sum_{n=1}^{\infty} \phi_n(x_i) Q_n e^{i\omega_s t} = e^{i\omega_s t} \sum_{k=1}^{\infty} \frac{F_j \phi_n(x_j) \phi_n(x_i)}{(\omega_n^2 - \omega_s^2) + i(2\xi_n \omega_n \omega_s)} \tag{4.}$$

One can observe that beam displacement is functions of modal parameters, i.e. ω_n, ξ_n and ϕ_n, as well as the harmonic force amplitude F_j, excitation frequency ω_s and its location x_j. The beam acceleration can also be obtained:

$$a(x_i,t) = a_i(t) = A e^{i\omega_s t} \tag{5.}$$

where

$$A = -\omega_s^2 \sum_{n=1}^{\infty} \frac{F_j \phi_n(x_j) \phi_n(x_i)}{(\omega_n^2 - \omega_s^2) + i(2\xi_n \omega_n \omega_s)} \tag{6.}$$

It is noted that in numerical simulation only *N* modes are included to calculate the beam acceleration.

2.2 Development of Harmonic Force Prediction Model

The conceptual diagram for force prediction model is depicted in Figure 2. For a structure subjected to unknown force, the sensor can detect the structural response as the input to the prediction model. Once the system modal parameters are also known, the force contents, including force amplitude and its location can be determined. This work deals with the prediction of unknown harmonic force acting on the cantilever beam. The accelerometer is employed to measure the beam response as the input to the prediction model. The system modal parameters, including natural frequencies, damping ratios and mode shapes, that can be determined theoretically or experimentally are also assumed known. The force prediction model will be developed to determine the force amplitude and its location, simultaneously. The optimization problem to predict the unknown harmonic force is formulated as follows:

Objective function:

$$Q_t = \sum_{r=1}^{N_t} \left[a_i(t_r) - \hat{a}_i(t_r)\right]^2 = \sum_{r=1}^{N_t} \left[-\omega_s^2 \sum_{n=1}^{\infty} \frac{F_j \phi_n(x_j) \phi_n(x_i)}{(\omega_n^2 - \omega_s^2) + i(2\xi_n \omega_n \omega_s)} e^{i\omega_s t_r} - \hat{a}_i(t_r) \right]^2 \tag{7.}$$

Design variables:

$$F_j, j \tag{8.}$$

When $j = 1$, $\phi_n(x_j)$ equal to $\phi_n(x_1), n = 1,2,...,N$, and etc. The objective function Q_t is defined as the sum of square errors between the measured acceleration $\hat{a}_i(t_r)$ and the predicted acceleration $a_i(t_r)$ over the time range from t_1 to t_{N_t}. As shown in Equation (5), the predicted acceleration $a_i(t_r)$ is functions of structural modal parameters and force contents. Structural modal parameter can be known. The unknown force contents are the force amplitude F_j and its location x_j, while the force excitation frequency ω_s can be easily detected. The design variables can then be identified as F_j and j. The index j related to the location x_j will result in $\phi_n(x_j), n = 1,2,...,N$. By the resolution of the optimization problem, the unknown harmonic force amplitude and its location index j can be determined simultaneously. The objective of the optimization problem is, therefore, to find F_j and j so as to minimize the sum of square errors between $\hat{a}_i(t_r)$ and $a_i(t_r)$.

III. Development of Prediction Program

The force prediction program is developed by Compaq Visual FORTRAN [14]. The optimization subroutine DBCPOL [15], which adopts direct search complex algorithm to solve general optimization problem with multiple design variables, is used to solve for the design variables, i.e. the force amplitude F_j and its location index j. The force prediction program flow chart is shown in Figure 3. There are two program options. Option (I) uses theoretically determined modal parameters and the specified harmonic force to generate the theoretical beam acceleration response to represent the measured response $\hat{a}_i(t_r)$ for the verification of the force prediction model. Option (II) deals with the experimental validation. Program will read in experimentally measured beam acceleration $\hat{a}_i(t_r)$ to predict the unknown applied harmonic force contents. Both theoretical and experimental prediction results will be presented in Section V.

IV. Experimental Setup

Table 1 shows the beam dimensions and its material properties. Conventional modal testing is carried out to obtain the beam modal parameters and validated with theoretical modal analysis. The test grid points on the beam are shown in Figure 1(b). The first four natural frequencies of bending modes and the corresponding damping ratios are listed in Table 2. The first four bending mode shapes are shown in Figure 4. As one can observe the modal parameters agree well between theoretical and experimental analysis.

Figure 5 shows the experimental layout for harmonic force prediction. The harmonic force is stimulated by the mini shaker (BK4810). Different force levels and excitation frequencies can be controlled by the signal generator (BK3016). The accelerometer (PCB352A10) is applied to measure the beam response $\hat{a}_i(t_r)$ due to the harmonic force excitation. The force amplitude F_j can be monitored through the force transducer (BK8200) connected to the dual channel analyzer (BK3550). The force prediction program is operated off-line to determine the force amplitude F_j and location index j with the input of $\hat{a}_i(t_r)$ and the determined structural modal parameters.

V. Results and Discussions

5.1 Theoretical prediction results – Option (I)

This section presents the theoretical prediction results by program Option (I). The measured acceleration is replaced by the theoretically generated response to validate the developed prediction model. Figure 6 shows the prediction results for different force amplitudes and locations. The excitation frequency is $f_1 < f_s = 30\text{Hz} < f_2$, between the first and second natural frequencies. Figure 6(a) shows the force amplitude prediction results. The horizontal axis is the number of iteration in solving the optimization problem. The vertical axis represents the force amplitudes. The legend (6,2) in Figure 6(a) denotes *i*=6, *j*=2, i.e. the force location at position 2 and the accelerometer at position 6. The harmonic forces are applied at position 2, 5, 10 and 15, respectively. The horizontal dash line in Figure 6(a) indicates the applied harmonic force amplitude. One can observe that the predicted force amplitudes converge to the actual values for the four cases. Figure 6(b) shows the predicted force location results. The vertical axis represents the position index *j*. As one can see, the force position index *j* also converges to the actual applied force location very well. Figure 7 show the similar prediction results to Figure 6 except that the excitation frequency is $f_s = 14.01\text{Hz} \approx f_1$, i.e. close to the first natural frequency. Both harmonic force amplitude and its location index converge to the actual values very well too. The force prediction model works

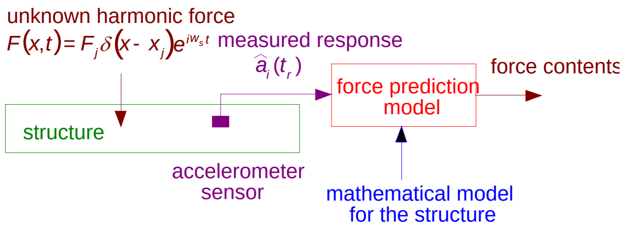

Figure 2. Conceptual diagram for force prediction

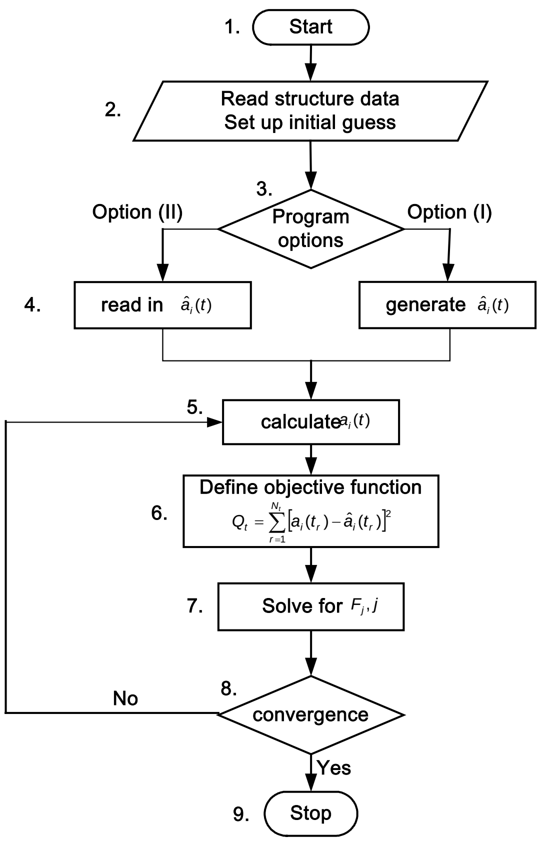

Figure 3. Force prediction program flowchart

Table 1. Beam dimensions and material properties

Material	Steel
Length (L_b)	0.3 m
Width (b_b)	0.0394 m
Thickness (t_b)	0.0016 m
Density (ρ_b)	7870 kg/m3
Young's Modulus (E_b)	207×109 N/m2
Poisson ratio (υ_b)	0.292

Table 2. Natural frequencies and damping ratios of cantilever beam

Mode	Experimental (Hz)	Theoretical (Hz)	Error (%)	Damping ratio (%)
1	14.01	14.728	-4.87	1.3478
2	90.39	92.298	-2.06	1.123
3	253.68	258.43	-1.83	0.455
4	497.07	506.46	-1.85	0.3957

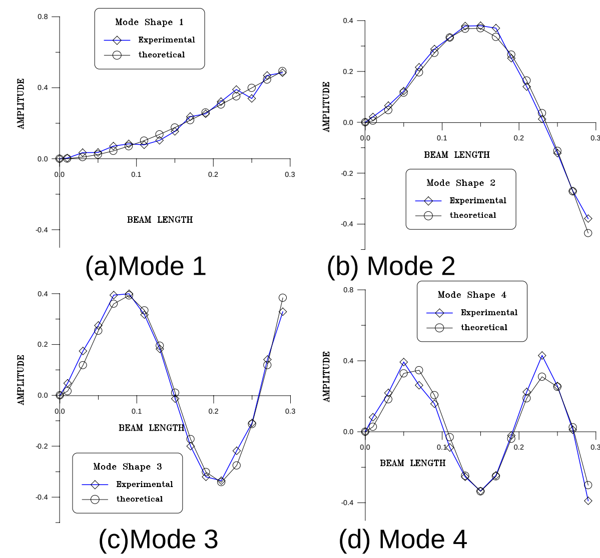

Figure 4. mode shapes of cantilever beam

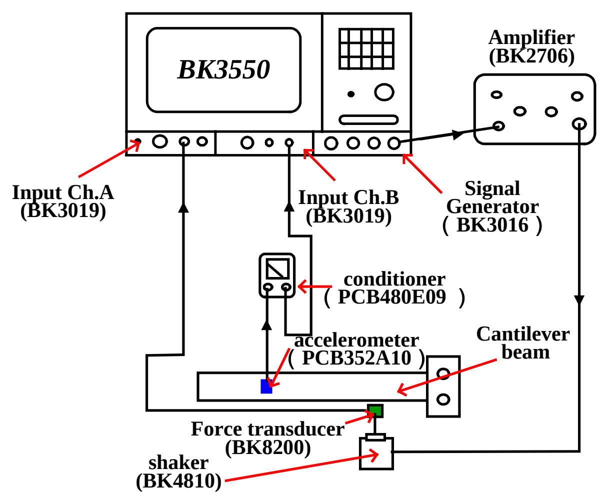

Figure 5. Experimental setup for harmonic force prediction

well for different force amplitudes and force locations as well as different excitation frequencies.

It is also interested to know the effect of sensor locations. Figures 8 and 9 show the theoretical prediction results considering different sensor location at positions 1, 5, 10 and 12 for off-resonance excitation ($f_1 < f_s = 30\text{Hz} < f_2$) and on-resonance excitation ($f_s = 14.01\text{Hz} \approx f_1$), respectively. Figure 8(a) shows the force amplitudes converge to the applied force levels very well except for the case (*i*,*j*)=(10,15) with triangle symbol. In Figure 8(b), the predicted force location is also exactly correct except the case (*i*,*j*)=(10,15) converging to *j*=14. This can be the cause that the

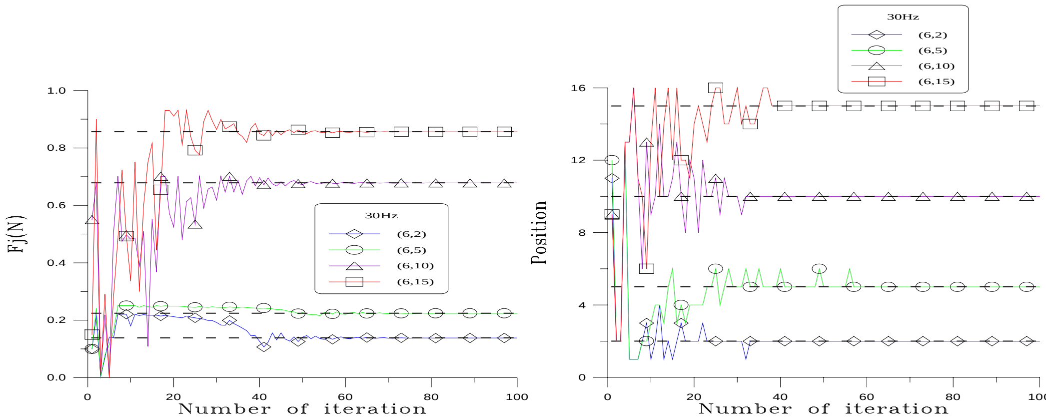

(a) force amplitude **(b) force location**

Figure 6. Option (I): prediction results for different force amplitudes and locations, $f_1 < f_s = 30\text{Hz} < f_2$

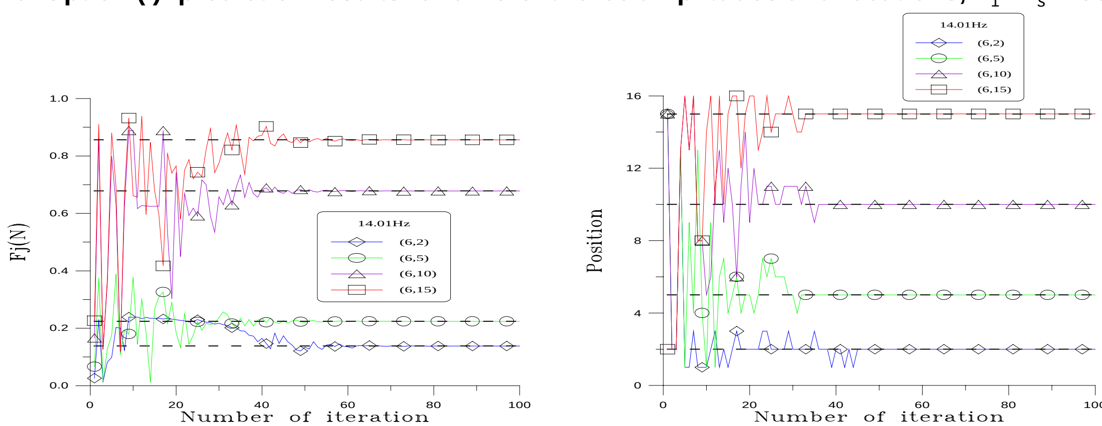

(a) force amplitude **(b) force location**

Figure 7. Option (I): prediction results for different force amplitudes and locations, $f_s = 14.01\text{Hz} \approx f_1$

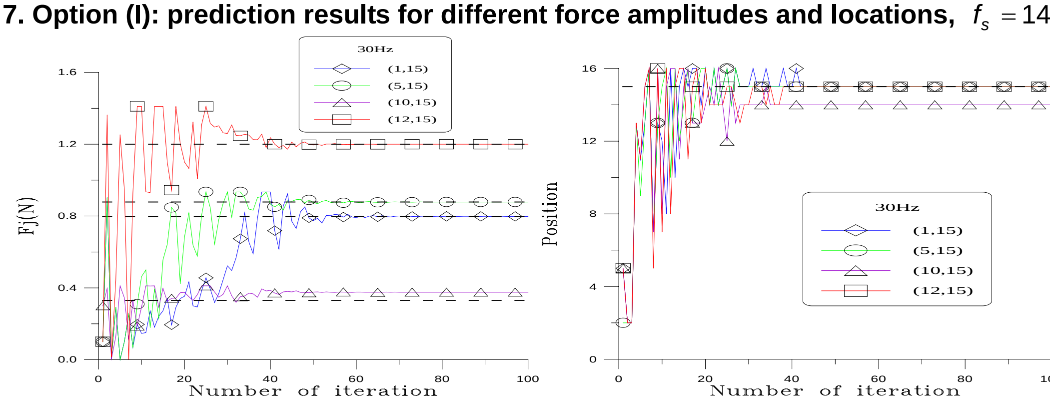

(a) force amplitude **(b) force location**

Figure 8. Option (I): prediction results for different sensor locations, $f_1 < f_s = 30\text{Hz} < f_2$

sensor location i=10 is near the nodal point of the fourth mode shape as shown in Figure 4(d). Similar results can be observed in Figures 9(a) and 9(b) for force amplitude and location prediction, respectively. Only the case (i,j)=(12,15) with square symbol cannot converge to the correct values. It is the cause that the sensor location i=12 is also near the nodal point of the second mode shape as shown in Figure 4(b). It can be noted that with proper choice of accelerometer location the prediction model can well predict the harmonic force amplitude and location for different excitation frequency conditions.

5.2 Experimental prediction results – Option (II)

Previous section theoretically demonstrates the feasibility of the prediction model in determining the unknown

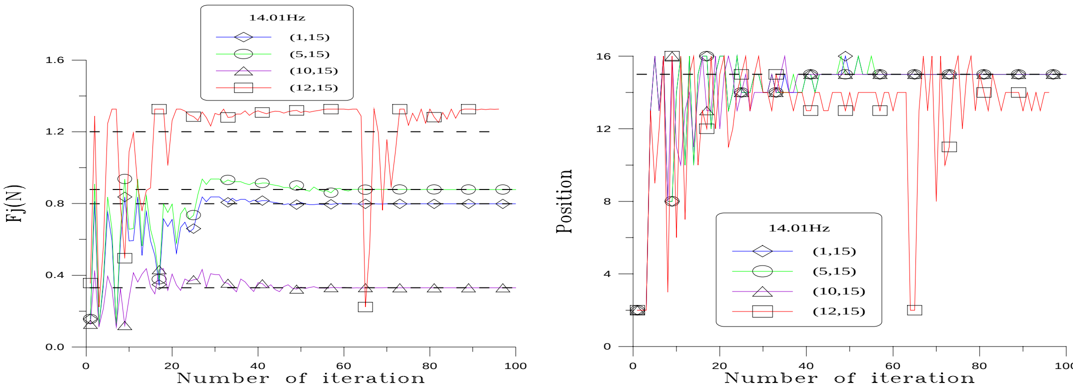

(a) force amplitude **(b) force location**

Figure 9. Option (I): prediction results for different sensor locations, $f_s = 14.01\text{Hz} \approx f_1$

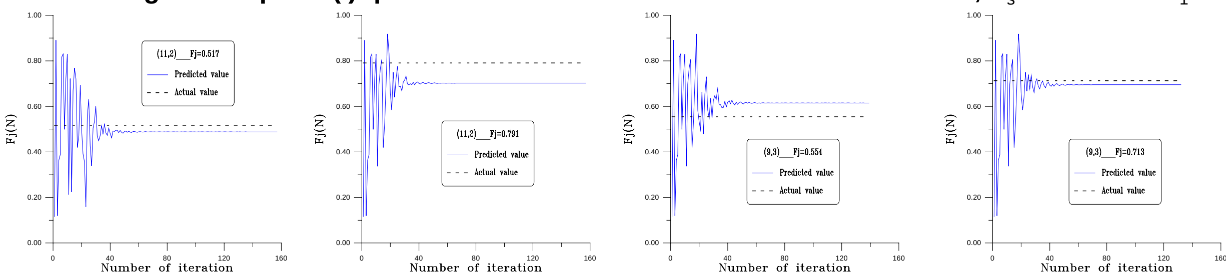

(a) (11,2), F_j =0.517 **(b) (11,2), F_j =0.791** **(c) (9,3), F_j =0.554** **(d) (9,3), F_j =0.713**

Figure 10. Option (II): force amplitude prediction convergence lines, $f_s = 14.01\text{Hz} \approx f_1$

Table 3. Option (II): prediction results for different force amplitudes, $f_s = 14.01\text{Hz} \approx f_1$

(i,j)	Actual Force Amplitude (N)	Predicted Force Amplitude (N)	Error (%)	Predicted Force Location
(11,2)	0.517	0.488	-5.61	2
(11,2)	0.791	0.702	-11.25	2
(9,3)	0.554	0.615	11.01	3
(9,3)	0.713	0.695	-2.52	4

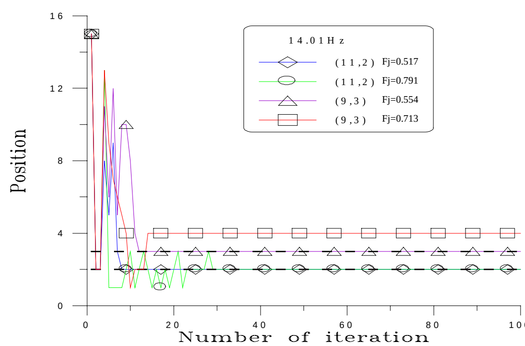

Figure 11. Option (II): prediction results for different force amplitudes and locations, $f_s = 14.01\text{Hz} \approx f_1$

harmonic force amplitude and its location simultaneously. This section will present the experimental prediction results. The experiments are as detailed in Section IV.

Table 3 shows the prediction results for different force amplitudes and locations, when $f_s = 14.01\text{Hz} \approx f_1$ near the first resonance excitation. Figure 10 shows the typical convergence curves for the predicted force amplitudes verse the number of iteration, and Figure 11 shows the predicted locations. As seen from Figure 10, the convergence curves vary up and down along the actual value and finally converge close to the actual force amplitudes. The prediction errors of force amplitudes as shown in Table 3 are within $\pm 12\%$. From Figure 11 and Table 3, the force location is shown correctly predicted except the case (*i*,*j*)=(9,3) with force amplitude F_j =0.713 N. However, the predicted location *j*=4 is near to the actual location *j*=3.

Table 4 and Figure 12 show more cases for different force locations. The sensor is fixed at position 12, and the harmonic forces are applied at positions 2, 3, 4 and 5, respectively. From Table 4, the maximum prediction error of force amplitude is 13.99% for (*i*,*j*)=(12,5). The location prediction can be very well as observed in Figure 12. There are about 50 iterations to get convergence solution for the case (*i*,*j*)=(12,2) with diamond symbol in Figure 12. The

Table 4. Option (II): prediction results for different force locations, $f_s = 14.01\text{Hz} \approx f_1$

(i,j)	Actual Force Amplitude (N)	Predicted Force Amplitude (N)	Error (%)	Predicted Force Location
(12,2)	4.5	3.998	-11.16	2
(12,3)	0.696	0.718	3.16	3
(12,4)	0.495	0.518	4.65	4
(12,5)	0.0772	0.088	13.99	5

Table 5. Option (II): prediction results for different sensor locations, $f_s = 14.01\text{Hz} \approx f_1$

(i,j)	Actual Force Amplitude (N)	Predicted Force Amplitude (N)	Error (%)	Predicted Force Location
(15,3)	0.556	0.398	-28.42	3
(12,3)	0.772	0.9476	22.75	3
(8,3)	0.682	0.915	34.16	3
(5,3)	0.59	0.715	21.19	3

Table 6. Option (II): prediction results for different excitation frequencies

(*i,j*)	Excitation Frequency (Hz)	Actual Force Amplitude (N)	Predicted Force Amplitude (N)	Error (%)	Predicted Force Location
(5,3)	14.01	0.681	0.7115	4.48	3
(8,2)	52	0.117	0.1215	3.85	2
(12,2)	90.73	0.402	0.488	21.39	2
(15,3)	253.45	0.385	0.415	7.79	3

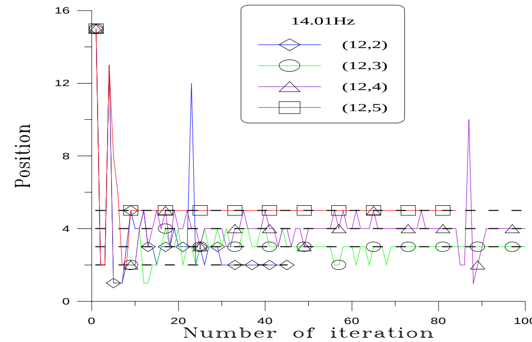

Figure 12. Option (II): prediction results for different force locations, $f_s = 14.01\text{Hz} \approx f_1$

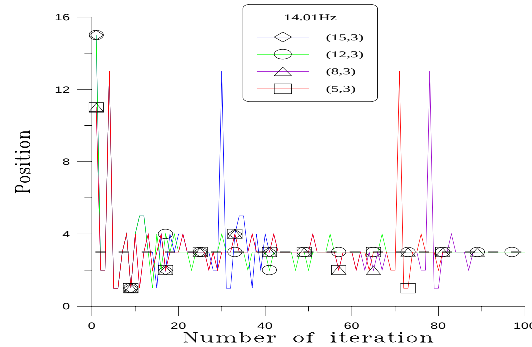

Figure 13. Option (II): prediction results for different sensor locations, $f_s = 14.01\text{Hz} \approx f_1$

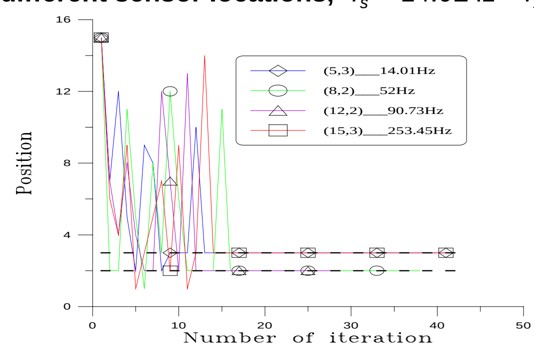

Figure 14. Option (II): prediction results for different excitation frequencies

prediction model is, therefore, validated for different force amplitudes and locations.

It is also interesting to study the effect of sensor location on the prediction model. Table 5 and Figure 13 show the predictions results. Although there are about 20-30% errors in the amplitude prediction, the location prediction is exactly correct. The experimental errors are considered in a reasonable range. Finally, Table 6 shows the prediction results for different excitation frequencies. The amplitude prediction errors are within 8% except the case (i,j)=(12,2) about 21%. Figure 14 shows the convergence curve for the predicted location index verse the number of iteration. One can see that the location prediction is exactly correct. In summary, the prediction model works reasonably well in actual experimental verification for different force amplitudes, locations and excitation frequencies as well as different sensor locations.

VI. Conclusions

This paper develops the unknown harmonic force prediction algorithm applied to cantilever beam structure. The prediction model can predict the harmonic force amplitude and its location simultaneously. Both theoretical and experimental force prediction results are presented to validate the prediction model. Some conclusions are made as follows:

1. The prediction model is well validated through the numerical simulation and successfully predicts the harmonic force amplitude and its location.
2. In actual experimental prediction, the force amplitude can be reasonably predicted as well as the force location.
3. The effects of different force amplitudes, locations and excitation frequencies on the prediction model are also studied. With the proper selection of sensor location the prediction model can work reasonably well.
4. The developed harmonic force prediction methodology can also be extended to other engineering structures as well as employing different sensors.

VII. Acknowledgement

The authors gratefully thank the financial support of this work from National Science Council, TAIWAN under the contract number: NSC92-2212-E-020-006.

VIII. Reference

1. Stevens, K. K., 1987, “Force Identification Problems – an Overview,” *Proceeding of the 1987 SEM Conference on Experimental Mechanics*, June, pp. 838-844.
2. Wang, B. T., 2002, “Prediction of Impact and Harmonic Forces Acting on Arbitrary Structure: Theoretical Formulation," *Mechanical Systems and Signal Processing*, Vol. 16, No. 6, pp. 935-953.
3. Verhoeven, J., 1988, "Excitation Force Identification of Rotating Machines Using Operational Rotor/Stator Amplitude Data and Analytical Synthesized Transfer Functions," *ASME Journal of Vibration, Acoustics, Stress, and Reliability in Design*, Vol. 110, pp. 307-314.
4. Vyas, N. S., and Wicks, A. L., 2001, “Reconstruction of Turbine Blade Forces from Response Data,” *Mechanism and Machine Theory*, Vol. 36, pp. 177-188.
5. Karlsson, S. E. S., 1996, “Identification of External Loads From Measured Harmonic Responses,” *Journal of Sound and Vibration*, Vol. 196, No. 1, pp. 59-74.
6. Moller, P. W., 1999, “Load Identification Through Structure Modification,” *Transactions of the ASME Journal of Applied Mechanics*, Vol. 66, pp. 236-241.
7. Wu, E., Yeh, J. C., and Yen, C. S., 1994, “Identification of Impact Forces at Multiple Locations on Laminated Plates,” *AIAA Journal,* Vol. 32, No. 12, pp. 2433-2439.
8. Choi, K., and Chang, F. K., 1996, “Identification of Impact Force and Location Using Distributed Sensors,” *AIAA Journal*, Vol. 34, No. 1, pp. 136-143.
9. Doyle, J. F., 1994, “A Genetic Algorithm for Determining the Location of Structural Impacts,” *Experimental Mechanics*, Vol. 34, No. 3, pp. 37-44.
10. Martin, M. T., and Doyle, J. F., 1996, “Impact Force Identification from Wave Propagation Responses,” *International Journal of Impact Engineering*, Vol. 18, No. 1, pp. 65-77.
11. Martin, M. T., and Doyle, J. F., 1996, “Impact Force Location in Frame Structures,” *International Journal of Impact Engineering*, Vol. 18, No. 1, pp. 79-97.
12. Wang, B. T., and Chui, T. S., 2003, “Determination of Unknown Impact Force Acting on Simply Supported Beam,” *Mechanical Systems and Signal Processing*, Vol. 17, No. 3, pp. 683-704.
13. Meirovich, L., 1967, *Analytical Methods in Vibrations*, Macmillan Publishing Co., Inc., New York.
14. Compaq Computer Corporation, 2001, Compaq Visual Fortran Version 6.6, Houston, Texas.
15. Visual Numerics, Inc., 1997, *IMSL Fortran Subroutines for Mathematical Applications,* Vol. 1 and 2, Visual Numerics, Inc.